Scientific Research Publishing

Open Journal of Geology, 2023, 13, 828-846
https://www.scirp.org/journal/ojg
ISSN Online: 2161-7589
ISSN Print: 2161-7570

An Orthogonal Collision Dynamic Mechanism of Wave-Like Uplift Plateaus in Southern Asia

Weihong Qian[1,2*], Jeremy Cheuk-Hin Leung[1], Banglin Zhang[1]

[1]Guangzhou Institute of Tropical and Marine Meteorology, CMA, Guangzhou, China
[2]School of Physics, Peking University, Beijing, China
Email: *qianwh@pku.edu.cn

How to cite this paper: Qian, W.H., Leung, J.C.-H. and Zhang, B.L. (2023) An Orthogonal Collision Dynamic Mechanism of Wave-Like Uplift Plateaus in Southern Asia. *Open Journal of Geology*, **13**, 828-846.
https://doi.org/10.4236/ojg.2023.138037

Received: June 30, 2023
Accepted: August 15, 2023
Published: August 18, 2023

Abstract

In southern Asia, there are three large-scale wave-like mountains ranging from the Tibetan Plateau westward to the Iranian Plateau and the Armenian Plateau. On the southern side between plateaus, there are the Indian Peninsula and the Arabian Peninsula. What dynamic mechanisms form the directional alignment of the three plateaus with the two peninsulas remains a mystery. In the early stages of the Earth's geological evolution, the internal structure of the Earth was that the center was a solid core, and the outmost layer was a thin equatorial crust zone separated by two thick pristine continents in polar areas, while the middle part was a deep magma fluid layer. Within the magma fluid layer, thermal and dynamic differences triggered planetary-scale vertical magma cells and led to the core-magma angular momentum exchange. When the core loses angular momentum and the magma layer gains angular momentum, the movement of upper magma fluids to the east and the tropical convergence zone (TCZ) drives the split and drift of two thick pristine continents, eventually forming the current combination of these plateaus and peninsulas and their wave-like arrangement along the east-west direction. Among them, the horizontal orthogonal convergence (collision) of upper magma fluids from the two hemispheres excited the vertical shear stress along the magma TCZ, which is the dynamic mechanism of mountain uplifts on the north side and plate subductions on the south side. To confirm this mechanism, two examples of low-level winds are used to calculate the correspondence between cyclone/anticyclonic systems generated by the orthogonal collision of airflows along the atmospheric TCZ and satellite-observed cloud systems. Such comparison can help us revisit the geological history of continental drift and orogeny.

Keywords

Plateau Uplift, Plate Subduction, Tibetan Plateau, Iranian Plateau, Armenian Plateau

1. Introduction

The Tibetan Plateau in southern Asia is known as the roof of the world. However, it does not exist in isolation, with the Iranian Plateau and the Armenian Plateau lined up on its western side [1]. On the southern side between these three plateaus are the Indian Peninsula and the Arabian Peninsula. Synoptically, the area of southern Asia is under the tremendous attack of compressive forces from surrounding regions, which has caused tight folding and resulted in wave-like structure of topography. It has an acute nose of waves in the western Tibetan Plateau. The adjacent Iranian Plateau in the west has an open saddle, whereas it further in the west Armenian Plateau is an open vertex with smooth convexity. As compared to the Tibetan Plateau, the Armenian Plateau and the Iranian Plateau are relatively open under less stress. The intensity of stress in the western Tibetan Plateau is high, which further in the east, ease out and became open and flat. Visually, the resultant forces of this compressive system pushed the Tibetan Plateau and the Armenian Plateau towards the North and the Iranian Plateau towards the south. Historically, most earthquakes occurred along the wave-like tectonic belt. This complex tectonic environment has severely affected the drainage evolution and valley development sequence of the various basins of the Indian Himalayas and the fluvial terraces since the Quaternary Period [2] [3]. There are many sensory descriptions that require a theory to confirm. First, what dynamic mechanisms form this wave-like structure of topographical uplift remains a mystery.

There are two main hypotheses about the uplift cause of mountains or plateaus, which are continental collision and mantle plume. The most widely accepted hypothesis is that the uplift of the Tibetan (Iranian) Plateau is primarily a result of the collision between the Indian (Arabian) and Eurasian tectonic plates [4] [5] [6] [7]. It is believed that around 50 million years ago, the Indian Subcontinent began colliding and subducting with the Eurasian Plate, leading to the gradual uplift of the Tibetan Plateau [8] [9]. This hypothesis explained mountain uplift through the convergence or collision of tectonic plates has some limitations. While this process can lead to the uplift of mountain ranges, such as the effect of continental collision in southern Asia, the specific mechanisms of crustal thickening and mountain building within the collision zone are not fully understood [10]. Questions include how rapidly suturing taken place, what extent the collision of continents affects plate motion, how much shortening of continental crust occurs, how this shortening occurs and how it is distributed in space. Although continental collision can provide a broad framework for understanding mountain uplift, it does not offer precise predictability of the exact locations and characteristics of mountain ranges. Therefore, this hypothesis is difficult to precisely determine the relationship between tectonic events and orogenic times. Fundamentally, it does not explain the whereabouts of the Indian plate before this time, nor does it explain what the force of the Indian plate drifting northward is and what the mechanism of the Indian plate sinking under the Eurasian plate is.

The mantle plume hypothesis proposes that there are localized upwellings of abnormally hot and buoyant material from the Earth's mantle to the surface. According to this hypothesis, these plumes of molten rock, or magma, rise from deep within the mantle and can produce volcanic activity at the Earth's surface. The mantle plume hypothesis suggests that these plumes are relatively stationary, while the tectonic plates move above them. There are many studies on the roles of mantle plumes and remnants in the uplift of the Tibetan Plateau [11] [12] [13]. One limitation of the hypothesis is the lack of direct observational evidence such as detailed physical structures for mantle plumes because they are inferred based on surface features such as volcanic activity and hotspot tracks [14] [15]. While mantle plumes can contribute to localized uplift in volcanic regions, they are not considered a primary mechanism for the uplift of entire mountain ranges. The relatively slow uplift rates associated with mantle plumes are insufficient to explain the rapid and large-scale uplift observed in many mountain ranges. On the other hand, the presence and significance of mantle plumes are still a subject of scientific debate because there is a geological controversy between plate and plume hypotheses [16] [17].

In addition to the two main mountain uplift hypotheses mentioned above, there are other hypotheses, such as the climate-driven hypothesis. The influence of climate drives on mountains comes mainly from external (surface) processes such as airflows and water flows. However, this hypothesis is highly controversial [18] [19] [20] [21]. Does plateau uplift affect the climate (monsoon), or does a change in climate cause the plateau uplift? The prevailing opinion assigns that the Tibetan Plateau plays a crucial role in shaping the Asian climate. The opposite view is that climate change alters the load on the plateau through erosion and changing alpine glaciation (ice sheets), causing the plateau to rise again. The reason for this controversy comes from the lack of sufficient observational data and judgment of geopotential energy sources. Climate change is an event that occurs in the atmosphere and hydrosphere, while plateau uplift is an event that occurs on the Earth's crust. The altitude (geopotential energy accumulation relative to sea level) of the latter can only be explained by the dynamics of the Earth's interior. So, we should go back to the first two hypotheses. Continental collisions and mantle plumes (volcanic activity) are traces of crustal activity left on the Earth's surface during geological periods. They are all dynamic interactions that occur inside the Earth. The former is a large-scale horizontal action, and the latter is a vertical action on a local scale.

The previous views believe that the uplift of the Tibetan Plateau is a complex and ongoing geological process that occurred over a considerable span of time. The timescales vary depending on the specific geological processes being considered. The major uplift of the Tibetan Plateau is attributed to the collision between the Indian Subcontinent and the Eurasian Plate, which began in the Cenozoic Era, approximately 66 - 55 million years ago [6] [22]. The initial stages of uplift are thought to have started during the Eocene epoch (56 - 34 million years ago) and continued into the Miocene epoch (23 - 5 million years ago) [23]. The

most significant uplift and crustal thickening of the Tibetan Plateau are believed to have occurred during the late Miocene epoch and have continued into the present [24]. It was believed that this period corresponds to the intensification of the collision between the Indian and Eurasian plates, resulting in the formation of the highest peaks in the Tibetan Plateau, including the Himalayas. The Quaternary Period, which encompasses the past 2.6 million years, is characterized by alternating glacial and interglacial periods as the climate-driven uplift hypothesis [25]. These climatic cycles have also influenced the uplift of the Tibetan Plateau. The above time traceback is largely shorter than several billion years and is not associated with the formation and breakup of supercontinents. We believe that the process of supercontinent assembly and dispersal such as Pangaea and Gondwana should also form the uplift of mountains, particularly the formation of plateaus in southern Asia.

Considering the internal dynamics of the early Earth, we study how large-scale horizontal motion energy inside the Earth can be regionally converted into vertical convective motion energy (mountain uplift). In our recent article on continental drift and orogeny [26], the study time traceback forwards to the early Earth about 4.54 billion years ago in the formation of the Earth's pristine crust, spatially considering the relative motion of the upper magma fluids caused by the exchange of angular momentum between the inner solid core and the outer magma layer. During the early geological evolution of the first loss of angular momentum in the core and the angular momentum gained by magma, the primordial continents formed at the middle and high latitudes of the two poles separated due to the eastward movement of magma fluids and the effect of Coriolis force towards the equator. The separated continental plates in the Northern Hemisphere drifted southeastward while the plates in the Southern Hemisphere drifted northeastward. Finally, continental plates drift from both hemispheres to the tropical convergence zone (TCZ) and an orthogonal collision occurs. Orthogonal collisions between continental plates driven by the horizontal motion of magma fluids can create shear stresses perpendicular to the ground. The two directions of shear stress can explain the uplift of the Tibetan Plateau on the northern side and the subduction of the continental plate on the southern side. Therefore, the purpose of this paper is to use such shear stresses in Section 2 to explain the uplifted dynamics of not only the Tibetan Plateau, but also the Iranian Plateau and the Armenian Plateau in detail. Section 3 gives the dynamics of the formation of multiple vortex cloud systems on the Pacific atmospheric TCZ. Section 4 compares the similarities between the southern Asian plateaus and the anomaly cloud systems along the Pacific TCZ. To demonstrate the effect of shear stress, Section 5 specifically calculates two temporal examples of vortex cloud systems formed by the updraft on the Pacific atmospheric TCZ. Finally, results and discussion are given in Section 6.

2. Wave-Like Plateau Belt in Southern Asia

Geographically, the southern part of Asia is divided into three regions: Southeast

Asia, South Asia, and Southwest Asia. Southeast Asia includes the Sino-Indian Peninsula and islands around the South China Sea, so that the geomorphology is dominated by peninsulas and islands. South Asia is dominated by the Indian Peninsula, including neighboring Pakistan, Bangladesh, and Sri Lanka. But the topography of South Asia includes the Tibetan Plateau in southwestern China and the Deccan Plateau on the Indian Subcontinent. Among them, the Tibetan Plateau is the largest and highest plateau in the world. Southwest Asia includes the Iranian Plateau in the north and the countries west of it, while the main body of the south is the Arabian Peninsula. The alpine terrain of Southwest Asia mainly includes the Iranian Plateau, the Arabian Plateau, and the Armenian Plateau.

In Figure 1, the red dotted line indicates the location of the tropical convergence zone (TCZ) of the upper magma fluids early in the Earth's geological evolution. This convergence zone running approximately east-west orientation in southern Asia is a part of the entire TCZ along the intertropical circle [26]. The terrain on its north side is tall while the terrain on its south side is topographic troughs or low-lying zones. In South Asia, the low-lying zone near the TCZ separates the Tibetan Plateau on the north side from the Deccan Plateau on the south side. In Southwest Asia, low-lying zones near the TCZ separate the Iranian Plateau and Armenian Plateau on the north side from the Arabian Plateau on the south side. On the north side of the TCZ, from east to west, the Tibetan Plateau, the Iranian Plateau, and the Armenian Plateau show a step-like distribution or fluctuating distribution in terms of topographic height. On the entire Eurasian territory north of the TCZ, the tall and broad mountainous plateaus are located on the Tibetan Plateau and extended northeastward to Lake Baikal in the Far East. Geomorphologically, it is obviously impossible to explain such a wide and tall topographic formation by the subduction of the Indian Plate to the

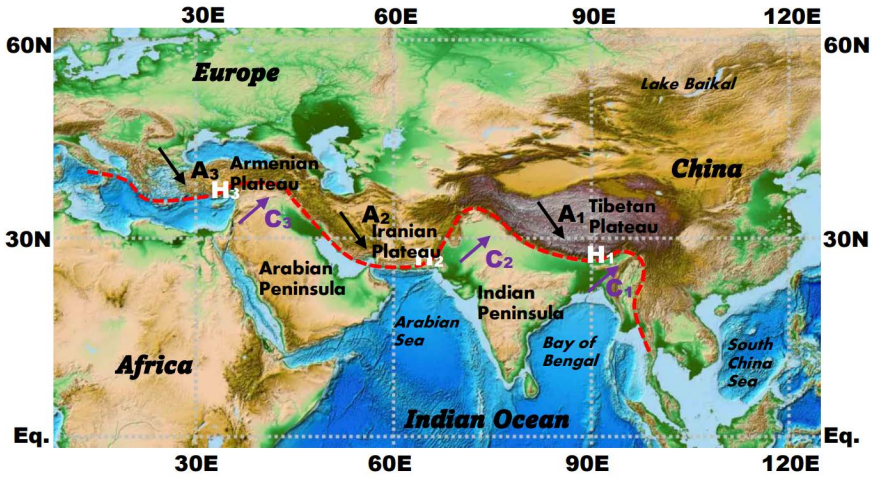

Figure 1. Three plateaus (A_1 - A_3) formed on the north side of magma-fluid tropical convergence zone (red dashed line) in southern Asia. The letters C_1 - C_3 indicate the three topographic troughs or low-lying zones, and the letters H_1 - H_3 indicate the three orthogonal convergence (collision) points formed by the magma fluid motions (arrows) on both sides of the convergence zone.

Asian Plate. Moreover, there are many fluctuations in the terrain from the Tibetan Plateau to Lake Baikal.

If the formation of the Iranian Plateau and the Armenian Plateau is explained by the subduction of the Arabian Plateau, then the Arabian Plateau has undergone clockwise and counterclockwise rotations. So how can it explain the formation of the Red Sea to the south and the Persian Gulf to the north? Interestingly, there were at least three fluctuations on this convergence zone in Asia. The three-southward wave-like bends along the convergence zone are indicated by the black arrows and the letter A in **Figure 1**. The three-northward wave-like bends along the convergence zone are indicated by the purple arrows and the letter C. In this way, the three plateaus in southern Asia are well indicated by the three wave-like bends.

According to our recent article [26], the Tibetan Plateau was formed at the beginning of Earth's geological evolution. At that time, the original crust was thin. The Earth's crust and the separated continental plates floated on top of the magma fluids. The collision of Asian continental plates with the Indian Plate near the convergence zone has resulted in the subduction of the southern plates and the uplift of the northern plates. This new crust, which is locally thickened, will provide an equilibrium on the magma fluids. The balance is expressed in the fact that the higher the mountain terrain on the ground, the deeper the embedded in the magma. It is the so-called, how high a mountain is, how deep its root is. Therefore, the three wave-like plateaus protruding from the surface of southern Asia correspond to the three wave-like mountain roots in the upper magma layer. In this paper, the plate is defined as the continental crust above sea level.

According to the three tall topographic plateaus along the convergence zone in **Figure 1**, there are corresponding fluctuations in the movement of the upper magma fluids. As indicated by the three pairs of arrows, the moved directions of adjacent magma fluids on both sides of the convergence zone are orthogonal. This phenomenon shows that there is a story in the history of geological evolution. The Tibetan Plateau, the Iranian Plateau and the Armenian Plateau may be traces left by the interaction of continental plates which were driven by magma fluids. Obviously, the thermal drive caused by the radioactive decay of local Earth's internal material and the dynamic drive of local mantle convection are difficult to explain the topographic wave-like phenomenon of this arrangement.

3. Dynamics of Wave-Like Vortex Cloud Systems

The three plateaus in southern Asia are left traces of geodynamics in geological history. It is difficult to infer the hierarchic events that have occurred in the history of the Earth from the traces (phenomena) left on the surface. To help understand possible orogenic events in geological history, we give a short time scale when one can observe and recognize events that occur with clouds and precipitation in atmospheric motion. Although the two types of events occur on different timescales and their compositions of matter are also different, we will see that they are both phenomena that occur in Earth's fluids.

Figure 2 is a cloud image of multi-satellite observations. The cloud system shown occurs in the eastern Pacific Ocean north of the tropical equator and south of Mexico. In the wide Pacific Ocean, the movement of the atmosphere is dominated by horizontal advection. The underlying surface of the atmosphere is a flat sea surface with no mountain terrain. If there is no influence of land-sea and mountain topography, the tropical convergence zone should be called the equatorial convergence zone. The northeasterly trade winds and the southeasterly trade winds on the ocean should converge on the equator. However, the long-observed convergence zone in climate is not along the equator, but around 8˚N - 10˚N in the eastern Pacific. This phenomenon has been explained by numerical model simulations [27] [28]. If the present-day terrain of the North and South American mountains is included, the tropical convergence zone simulated by the model is in the north of the equator on the eastern Pacific. When the mountain terrain of the North and South American continents is removed from the model, the resulting convergence zone is along the equator. This numerical experiment explains how the topography of mountains permanently alters the symmetrical motion of the tropospheric circulation relative to the equator. This simulation also suggests that the shift of the convergence zone in Figure 1 north of the equator is also the result of the movement of the upper magma fluids being influenced by the topographical roots of the thickened mountains.

Climatically, the eastern part of the tropical convergence zone is more northern position than that in western part. This phenomenon suggests that the location of the western convergence zone is relatively less affected by the topography of the mountain range in North and South America. The instantaneous fluctuations that occur in the convergence zone of horizontal airflows are called Rossby waves and are generated by the movement of the Earth's atmosphere relative to the rotation of the Earth. This wave-like moving phenomenon is related to the

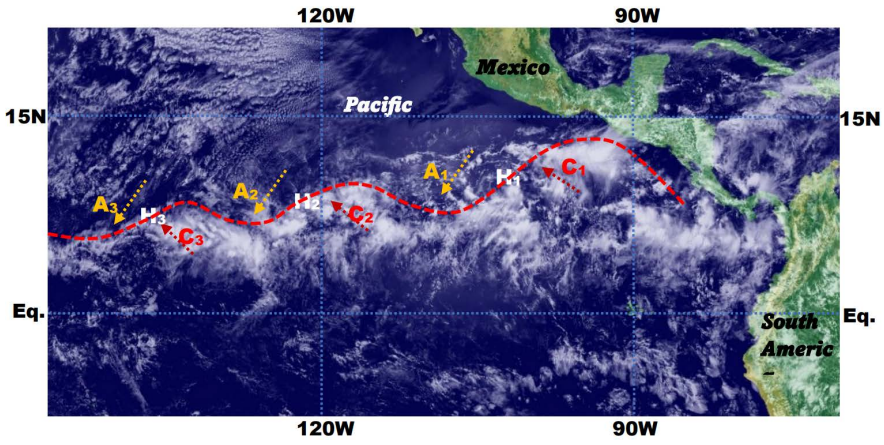

Figure 2. Cloud systems (white areas) combined by multiple polar-orbiting satellite observations. The letters C_1 - C_3 indicate cloud systems forming on the south side of the wave-like convergence zone (red dashed line), and the letters A_1 - A_3 indicate cloudless areas forming on the north side. Arrows indicate low-level atmospheric trade wind airflows coming from both sides of the tropical convergence zone.

Coriolis force. The Coriolis force is zero at the equator, so there are no fluctuations observed at the equator, and no typhoons and hurricanes are generated on the equator. The three wave-like cloud systems (letters C1, C2 and C3) in **Figure 2** are detected by satellites. Water vapor and heat are the highest on the equator due to more solar radiation. So, the three red arrows indicate the southeasterly warm-wet trade winds from the equator, while the three yellow arrows indicate the northeasterly cold-dry trade winds from higher latitudes. Affected by the Coriolis force in the Northern Hemisphere, the southeasterly warm-wet trade winds will produce cyclonic vortex, forming a low-pressure system. On the contrary, the northeasterly cold-dry trade winds will produce anticyclonic vortex, forming a high-pressure system. The low-pressure vortex corresponds to the convergence of airflows with clouds and rain. High-pressure system corresponds to the dispersion of airflows with clear or cloudless weather.

Multiple low-pressure vortices form near the tropical convergence zone, corresponding to the cloud and rain concentration area on the satellite cloud image. These contiguous low-pressure vortices and thermodynamic convective cloud systems are both hallmarks of the tropical convergence zone and bring heat and water vapor to the tropical convergence zone, forming planetary-scale updraft belts. This updraft radiates to both sides when it reaches the tropopause. Thus, a pair of Hadley cells are formed on both sides of the TCZ. The sinking airflows of Hadley cell form two cloudless high-pressure zones respectively near 15˚N and along the Equator in **Figure 2**. On the sea surface, the trade winds between the two high-pressure zones converge to form the tropical convergence zone. Interannual and decadal variations in the intensity of the Hadley cell exchange angular momentum between the Earth and the atmosphere through the frictional torque and the mountain torque [29] [30]. The Hadley gyre on both sides limits the transform of atmospheric mass and material crossing the convergence zone. Such vertical cell also exists in the magma fluids, so there is also an exchange of angular momentum between the core and the magma (or mantle) [31]. The mass and material including the continental plates on both sides of the magma-fluid convergence zone are equal. The timescale of core-magma angular momentum exchange is longer. The changes in the geomagnetic poles can be reflected and recorded in the abnormal geomagnetic polarities crossing the mid-ocean ridges [32]. The two Hadley cells in the atmosphere occur only in the troposphere of about 10 km thick, while the magma fluid layer in the early Earth was several thousand kilometers, so that the vertical cells in it had a planetary-scale structure.

The yellow and red arrows in **Figure 2** indicate the trade wind airflows near the sea surface, including the climatological trade wind airflows and the anomaly airflows. The trade wind airflows on both sides of the tropical convergence zone are orthogonally converged. The shear stress of the collision between them is [26],

$$\boldsymbol{\tau}_H = \left| \left(\frac{m_A}{r} v_A^2 \right) \cdot \left(\frac{m_B}{r} v_B^2 \right) \cdot \left(\boldsymbol{n}_A \times \boldsymbol{n}_B \right) \right|, \tag{1}$$

where the signs $\boldsymbol{n}_A$ and $\boldsymbol{n}_B$ are two-unit vectors of centripetal forces when airflows collide. The shear stress $\boldsymbol{\tau}_H$ is perpendicular to the plane formed by $\boldsymbol{n}_A \times \boldsymbol{n}_B$. Since $\boldsymbol{n}_A$ and $\boldsymbol{n}_B$ are parallel to the Earth's surface, the shear stress $\boldsymbol{\tau}_H$ is perpendicular to the Earth's surface and pointing up and down in two directions. In other words, the two directions of shear stress are an uplifting force and subducting force, respectively. The shear stress modulus is,

$$\tau_H = \left| \left(\frac{m_A}{r} v_A^2 \right) \cdot \left(\frac{m_B}{r} v_B^2 \right) \right| \sin\theta, \tag{2}$$

where, θ is the convergence or collision angle between two air parcels. It reaches the positive maximum when their collision angle is equal to 90˚ ($\sin 90^\circ = 1$) while it reaches the negative maximum when their collision angle is equal to 270˚ ($\sin 270^\circ = -1$). When they have an orthogonal collision with $\theta = 90$ degrees,

$$\tau_{HM} = \left| \left(\frac{m_A}{r} v_A^2 \right) \cdot \left(\frac{m_B}{r} v_B^2 \right) \right| = \left(m_A v_A^2 \right) \cdot \left(m_B v_B^2 \right) \Big/ r^2 . \tag{3}$$

Otherwise, when their collision angle is larger or less than 90˚, the shear stress modulus will be reduced.

4. Comparison of Wave-Like Systems in the Magma and Atmosphere

It is interesting to compare the wave-like terrain systems and wave-like cloud systems that appear in **Figure 1** and **Figure 2**, respectively. **Figure 1** reflects the traces left by the Earth's evolution to the present day, leaving traces of geological history. People have not experienced and are unlikely to experience in the future for the historical story shown in **Figure 1**. **Figure 2** is what happened in the atmosphere and is also a trace left over from atmospheric history. But the traces in **Figure 2** are stories or events that people can track and see again. Although numerical weather prediction models have been developed, the ability to predict tropical storm intensity is still not so high. The reason is that the dynamic fluid models that simulate atmospheric motion especially extreme events lack the core dynamic framework and physical parameters. For example, it is not clear why the downdrafts in the central eye area of the super-strong tropical storms (super typhoons and hurricanes) contrast so strongly with the updrafts in the surrounding cloud-rain walls. People do not even know the source of the huge energy in tornadoes. If there is no such principle and description of energy sources in the weather forecasting model, then how can extreme weather events of various storms be predicted?

In Equation (1), the left-hand side is the shear stress, which has magnitude and direction. On the right-hand side is the mass-energy density resulting from the collision of two air parcels (particles) or two magma blocks (continental plates). In high-energy physics, modern electron colliders use head-on or linear collisions that occur after accelerating electrons [33] [34]. A head-on collision of two particles is $\theta = 180$ degrees so that the shear stress modulus in Equation (2)

is zero. A head-on collision can make the energy of two particles linearly superimposed, but it cannot allow two old particles to collide to form a new physical state. It cannot also vertically change the moving direction of particles. The orthogonal collision of two particles can form a new physical state of matter that is completely different from the original particles [35]. This orthogonal collision is a one-way process in which mass is converted into energy in a thermonuclear reaction. Therefore, we use the sign "=|" instead of the symbol "=" in the three equations. In the two sides of the sign "=|", the values are equal, but there is no relationship of information exchange [36]. The two sides of the sign describe events that take place in two different worlds (universes).

Equation (2) indicates that two old objects can collide at different angles, producing positive or negative shear stress modulus. The shear stress modulus in which orthogonal collisions occur between substances is the largest. Equation (1) indicates that the new particles with high-energy density can move upward and downward perpendicular to the ground relative to the horizontal convergence or collision of air or magma parcels. This could explain why houses and trees that enter horizontally in a tornado are shredded and made vertically abandoned. A closer look at the enormous abnormal energy of the torn material movement in a tornado is clear [37].

Figure 1 shares many similarities with the events that occurred in **Figure 2**. The first similarity is that they both occur in the subtropical regions of the Northern Hemisphere, where magma fluids and atmospheric fluids are subjected to the same direction of Coriolis forces when they move relative to the Earth. The second similarity is that they are the same spatial scale and arrangement. The first difference is that the time scale is different, one is a historical event of nearly 100 million years, and the other is an event that can be repeated for several tens of hours. The second difference is that one is the magma fluids in the Earth's interior and the other is the atmospheric fluids. The third difference is their moving directions of magma fluids and atmospheric fluids on both sides of their tropical convergence zone. We believe that the collision of two-type Earth fluids on their tropical convergence zone follows the same law of Equation (1).

According to the law of Equation (1), the collision of airflows moving from near the equator towards the tropical convergence zone in the eastern Pacific Ocean with airflows coming from the north side will form a new vortex in which the updrafts will form clouds and cause rain. The result is several vortex cloud systems arranged along the tropical convergence zone and observed by satellites, as shown in **Figure 2**. In the vortex cloud system, there will also be violent updrafts and sinking airflows, so that the cloud system is not evenly distributed in space.

Similarly, according to the law of Equation (1), the three plateaus that appear on the current landscape of southern Asia and other surrounding geomorphological features can also be explained. In the early Earth stages of the geologic evolution, the upper magma fluids on the north side of the tropical convergence zone moved southeastward, splitting the pristine crust near the North Pole, and

driving the split continental plates to move southeastward. The upper magma fluids on the south side of the tropical convergence zone moved northeastward, splitting the pristine crust near Antarctica, and driving the split continental plates to drift northeastward. In the Southern Hemisphere, drifted plates include not only the Indian Plate and the Arabian Plate, but also the African Plate and the South American Plate. They all drifted simultaneously to reach the southern side of the tropical convergence zone. In the Northern Hemisphere, only the Eurasian Plate drifted southeastward to the place. The continental plates on either side of the tropical convergence zone were driven by the underlying magma fluids. The force of horizontal drift does not lie in the continental plate itself, but in the directional drive of the underlying magma fluids to the plate.

Both the Indian and Arabian plates are located on the northeast side of the Africa continental plate, while the islands of Southeast Asia are located on the southeast side of the Asian continental plate. Their current positions relative to the tropical convergence zone suggest that the directionality of continental drift is the result of underlying magma fluids driven. Under the continuous driving of the upper magma fluids, the African Continent with the Indian Plate and the Arabian Plate moved northeastward while the Eurasian Continent moved southeastward, so that we can explain the uplift of the Tibetan Plateau, the Iranian Plateau, and the Armenian Plateau. The energy of the three-plateau uplifts comes mainly from the continuous orthogonal collision of the underlying magma fluids. The geopotential height of current mountains above sea level is the geopotential energy stored by magma fluid collisions at that time. This large-scale geopotential energy of plateaus cannot be explained by the mantle plume hypothesis.

According to Equations (1) and (2), the two vertical convection directions of the shear stress and the positive or negative value of the shear stress modulus determine where plateaus rise and where plates subduct. Based on the totality of the initial Eurasian Continent drift and the totality of the initial African Continent drift with surrounding islands (or peninsulas), it is easy to explain the multiple topographic fluctuations and energy sources that occurred between the Tibetan Plateau and Lake Baikal. In this wide region, there is concentrated anomaly energy from the horizontal relative motion collision of continental plates, as well as is concentrated anomaly energy from the horizontal relative movement of the upper magma fluids.

Over the hundreds of millions of years since the onset of geological evolution, the core-magma angular momentum exchange has led to multiple-time changes in the direction of magma fluid motions. During the first accelerated rotation of the core, the magma fluids moved westward and poleward affected by the Coriolis force. Thus, the continental plates on both sides of the tropical convergence zone drifted westward and polar ward. The continental plate of Africa drifted southwestward to form the Mediterranean Sea. The main body of the Indian Plate is located on the tropical convergence zone due to that the northern part has undergone a subduction collision, so it has not left the southern edge of the

Asian continent. The Arabian Plate drifted southwestward, forming the Persian Gulf. The Red Sea is formed by the drift of the African Plate relative to the Arabian Plate driven by the upper magma fluids. From the back-and-forth drift of plates, the northwest side of the Arabian Plate drifted with less distance than that its southeast side relative to the tropical convergence zone. Morphologically, the Arabian Plate has a counterclockwise rotational drift relative to the northwest side.

Comparing the three cloud systems along the atmospheric tropical convergence zone in the eastern Pacific Ocean in **Figure 2**, we can look at the three plateaus arranged along the magma tropical convergence zone in southern Asia in **Figure 1**. The corresponding position (marked by C) of the three troughs in **Figure 1** resembles the three low-pressure circulation systems in **Figure 2**. The topographic valleys and plateaus appear in southern Asia. The high- and low-pressure circulation systems occur in the tropical Pacific Ocean. They all are the results or extreme events of orthogonal collision shear stress driven by different Earth's fluids. The similarity along the tropical convergence zone with the anomaly events occurred in **Figure 1** and **Figure 2** is not an accidental phenomenon, but the nature of fluid motion on the rotating Earth.

5. Calculation of Example Shear Stress Modulus

There are two types of meteorological satellites circling the Earth, the polar-orbiting satellites, and geostationary satellites. The latter is located above the equator and can continuously observe cloud systems within a certain range below the satellite. The polar-orbiting satellite orbits the Earth's north and south poles at relatively low altitudes, and the resolution of observations is high, but it is separated by several longitude black bands of cloud images as shown in **Figure 3(a)**. The combined cloud image in **Figure 3(a)** is the observed result of four times around the pole. There are four narrow black bands without being observed. **Figure 2** is a synthesis of observations from multiple polar-orbiting satellites. While it compensates for the black bands in **Figure 3(a)**, the need for correction and docking of data between different satellite observations also introduces errors.

Figure 3(a) is a polar-orbiting satellite cloud image observed around 18:00 UTC on 2 June 2021, which indicates the four cloud system positions C_1 - C_4. Correspondingly, four cloudless positions A_1 - A_4 are marked on the north side of the red dashed line. We hope to calculate the shear stress of the anomaly winds using the lower atmospheric airflows at the corresponding time and investigate the ability to indicate the cloud systems in **Figure 3(a)**. The winds used in this analysis with spatial resolution of 0.25 latitude-longitude degrees are downloaded from the fifth generation ECMWF atmospheric reanalysis (ERA5) data at 850 hPa at 18:00 UTC on 14 July 2020 and on 22 June 2021. The shear stress modulus of anomaly winds is calculated using Equation (2), taking the mass is 1 and considering the direction of the anomaly airflows. When two anomaly airflows converge towards a point, the shear stress modulus needs to

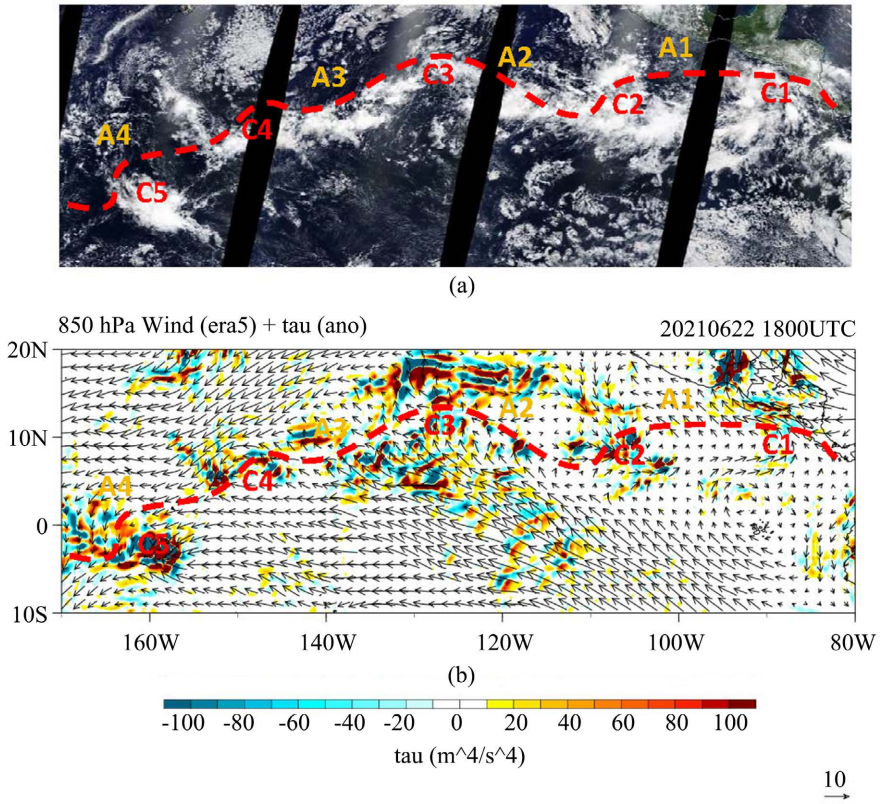

Figure 3. (a) Polar-orbiting satellite cloud image and (b) shear stress modulus (shading, $m^4 \cdot s^{-4}$) derived from 850 hPa anomaly winds at 18:00 UTC on 14 July 2020. In (a), the illustration is like in **Figure 2**. In (b), the red dashed line indicates the tropical convergence zone of observed winds at 850 hPa, and the letter C indicates the large center of shear stress modulus.

consider the angle between the two anomaly airflows. If the angle is less than 180 degrees, the shear stress modulus is a positive, otherwise, a negative if the angle is greater than 180 degrees. The positive and negative values of the shear stress modulus separate the directions of shear stress at that point. When the angle is 90 degrees (or 270 degrees), the shear stress modulus reaches the positive (or negative) maximum.

The hourly anomaly airflows or anomaly winds are calculated depending on the hourly climatological winds. The hourly climatology can be estimated by averaging reanalysis data for a variable v at time t (24 h a day) on calendar date d over M years,

$$\tilde{v}_d(\lambda,\varphi,p,t)=\frac{\sum_{y=1}^{M} v_{(d,y)}(\lambda,\varphi,p,t)}{M}, \tag{4}$$

where year y runs from 1 to M ($M \geq 30$ years), while λ, φ, and p denote longitude, latitude. and pressure level, respectively. When M is large enough, the estimated climatology should be a static state under thermodynamic equilibrium of the Earth-atmosphere system, which is only forced by the solar radiation and surface conditions [38]. The hourly climatology contains the diurnal cycle and

the annual cycle. Usually, the ERA reanalysis data are used with M = 30 years (1981-2010), which are available four times per day at 6-h intervals. Once the climatology is known, an anomaly $v'_{(d,y)}(\lambda,\varphi,p,t)$ can be extracted from a total or observed variable $v_{(d,y)}(\lambda,\varphi,p,t)$ by using Equation (4) and subtracting climatology $\tilde{v}_d(\lambda,\varphi,p,t)$. It also means that the observed variable is the sum of climatology and anomaly,

$$v_{(d,y)}(\lambda,\varphi,p,t)=\tilde{v}_d(\lambda,\varphi,p,t)+v'_{(d,y)}(\lambda,\varphi,p,t). \quad (5)$$

In **Figure 3(b)**, the black arrows indicate the observed wind direction, and the speed (arrow length) is given by the reanalysis data on the 850 hPa layer. The red dashed line is the tropical convergence zone of low-level observed winds. The shadow in **Figure 3(b)** is the shear stress modulus calculated by the anomaly winds using Equation (2). Four wave-like shading areas along the tropical convergence zone are the shear stress modulus generated by the collision of the anomaly airflows. In **Figure 3(b)**, the tropical convergence zone is well outlined the north boundary of cloud systems in **Figure 3(a)**. The four large centers of shear stress modulus calculated by the anomaly winds in **Figure 3(b)** correspond to the four cloud systems observed by the satellite in **Figure 3(a)**.

Figure 4 is another example of a cloud image and the shear stress modulus of anomaly winds at 18:00 UTC on 22 June 2021. From the polar-orbiting satellite cloud image (**Figure 4(a)**), there are five cloud systems (C_1 - C_5) located on the

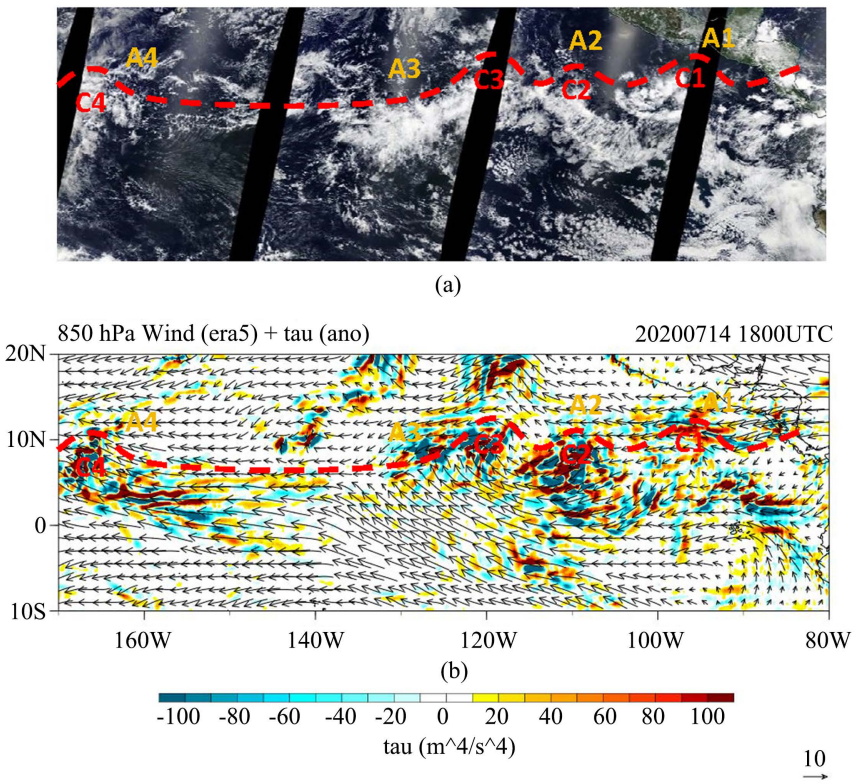

Figure 4. Same as **Figure 3**, but with (a) polar-orbiting satellite image and (b) 850 hPa shear stress modulus at 18:00 UTC on 22 June 2021.

south side of the red dashed line, while on the north side there are four cloudless areas (A_1 - A_4). The tropical convergence zone of observed airflows with five shading areas of shear stress modulus in **Figure 4(b)** is consistent with those outlined line of the satellite image in **Figure 4(a)**. Critically, the five centers of shear stress modulus calculated from the anomaly winds in **Figure 4(b)** provide a good indication of the five cloud systems observed by the satellite in **Figure 4(a)**. However, in some positions, the large shear stress modulus does not correspond completely to the cloud system, because the formation of cloud systems in the atmosphere is not only determined by the anomaly airflows at 850 hPa layer, but also related to the local atmospheric water vapor content. The results are better if we calculate and integrate shear stresses at multiple layers at each spatial point. Therefore, such dynamic mechanisms need to be introduced in future weather forecasting models.

Using the hourly observation of winds, we can determine the tropical convergence zone of the airflows in the Pacific Ocean, and we can also calculate the shear stress modulus of the anomaly winds using Equation (2). The large centers of the shear stress modulus correspond to the cloud systems on the satellite image. Therefore, during early geological evolution period, the current mantle should be the magma fluid layer of the Earth, leaving only the current crust and core as solid layers. Under such a vertical circle structure, using a similar atmospheric dynamic model and introducing the above dynamic mechanism of anomaly-fluid collision, we can also simulate the formation of three plateaus in southern Asia and the location of the southern valleys.

6. Results and Discussion

The Tibetan Plateau, the Iranian Plateau, and the Armenian Plateau, which have the highest east-west oriented elevations in southern Asia, are the result of the directional driving and the orthogonal colliding of the upper magma fluids in the early stage of the Earth's geological evolution. The geo-rotational deflection force caused by the eastward movement of the upper magma fluids has a component leaving the poles, so the magma fluids drive the pristine continent in the Northern Hemisphere to split and drift southeastward, and the pristine continent in the Southern Hemisphere to split and drift northeastward. When these continental plates drift to the tropical convergence zone, a continuous orthogonal collision occurs between the upper magma fluids and the plates from two sides at the same time. Since the location of the magma-fluid tropical convergence zone is located north of the equator, the results of the convergence or collision of continental plates form a series of wave-like plateaus on the north side of the tropical convergence zone and a series of wave-like valleys on the south side. According to the shear stress of the orthographic collision of magma fluids and continental plates, the geopotential energy of the orthographic collision is the greatest when the Tibetan Plateau is formed, so that the mountain range is the highest and the mountain root is the deepest. The fluid motion on both sides of

the magma-fluid tropical convergence zone has anomaly characteristics, showing local anomaly circulation in magma fluids. Multiple anomaly circulation systems in magma fluids are collided along large-scale convergence zones, resulting in the wave-like distribution of shear stress modulus. This explains the step-by-step and east-west oriented distribution from the Tibetan Plateau to the Iranian Plateau and the Armenian Plateau, which is also a stepwise distribution of geopotential energy.

There is a perennial convergence zone of lower atmospheric movements (southeasterly and northeasterly trade winds) in the tropical northeastern Pacific Ocean. In the tropospheric atmosphere over relatively flat oceans, there are anomalies superimposed on the climate trade winds in the atmospheric movement at each moment. Multiple cyclonic cloud systems will be arranged on the southern side of the tropical convergence zone, while multiple anticyclonic cloudless regions will be arranged on the northern side. The cloud systems observed by satellites are the product of anomaly energy release and water vapor condensation in the atmosphere under the orthogonal collision of anomaly airflows. According to the physical nature of shear stress, the result of orthogonal collisions of matter forms a new physical state. Therefore, the material composition of the Tibetan Plateau, the Iranian Plateau and the Armenian Plateau is no longer primitive continental crust material.

To confirm the above theoretical inference, we used the observed winds at 850 hPa to map the tropical convergence zone of the trade winds in the tropical Pacific Ocean and calculated the shear stress modulus of the anomaly winds. The calculations show that the intensity and location of the shear stress modulus of the anomaly airflows can indicate the wave-like cloud systems observed by satellites. The content of daily weather forecasts is to know the location and intensity of present and future cloud systems. These cloud systems that occur in the atmosphere are like a series of plateaus forming on the Earth's surface. In the early stage of geological evolution, the orthogonal collision of anomaly magma fluids along the tropical convergence zone is also the fundamental dynamic mechanism of plateau topography formation. The directional movement of the upper magma fluids drove the separation of the two pristine continents near the two polar areas. Multiple reciprocating drifts of continental plates driven by magma fluids form orogeny at the edge of plates.

Based on the theoretical results and data calculation products in this paper, we hope to introduce the dynamic mechanism of anomaly airflow collision in the numerical weather prediction model. Models that introduce an orthogonal collision mechanism of airflows have the potential to simulate and predict various extreme weather events, especially the anomaly energy of extreme weather events. Similarly, orthogonal collisions of magma fluids need to be introduced into geodynamic models. Only in this way, one can simulate the plateaus, mountains and valleys formed in geological history, and truly reflect the historical geodynamic process of their formation. Only in this way, can the mechanism of orthogonal

collision dynamics be introduced into mantle convective models in the future to predict local earthquake and volcanic activity.

Acknowledgements

The authors wish to thank the anonymous reviewer for constructive suggestions and comments that have improved the paper. The authors also thank Drs. F. Han and H. M. Qian for constructive discussion. This work was supported by the Guangdong Basic and Applied Basic Research Foundation (Grant Number: 2020A1515110275), the Innovative R&D Project in Guangdong Province in China (Grant Number: 2019ZT08G669) and the National Natural Science Foundation of China (Grant Number: 41775067).

Conflicts of Interest

The authors declare no conflicts of interest regarding the publication of this paper.

References

[1] Neill, I., Meliksetian, K., Allen, M.B., Navasardyan, G. and Kuiper, K. (2015) Petrogenesis of Mafic Collision Zone Magmatism: The Armenian Sector of the Turkish-Iranian Plateau. *Chemical Geology*, **403**, 24-41. https://doi.org/10.1016/j.chemgeo.2015.03.013

[2] Phartiyal, B. and Kothyari, G.C. (2012) Impact of Neotectonics on Drainage Network Evolution Reconstructed from Morphometric Indices: Case Study from NW Indian Himalaya. *Zeitzchrift Fur Geomorphologie*, **56**, 121-140. https://doi.org/10.1127/0372-8854/2011/0059

[3] Kumar, A., Srivastava, P. and Devrani, R. (2020) Using Clast Geometries to Establish Paleoriver Discharges: Testing Records for Aggradation and Incision from the Upper Indus River, Ladakh Himalaya. *Geomorphology*, **362**, Article ID: 107202. https://doi.org/10.1016/j.geomorph.2020.107202

[4] Molnar, P. and Tapponnier, P. (1975) Cenozoic Tectonics of Asia: Effects of a Continental Collision. *Science*, **189**, 419-426. https://doi.org/10.1126/science.189.4201.419

[5] England, P. and Houseman, G. (1989) Extension during Continental Convergence, with Application to the Tibetan Plateau. *Journal of Geophysical Research*: *Solid Earth*, **94**, 17561-17579. https://doi.org/10.1029/JB094iB12p17561

[6] Rowley, D.B. (1996) Age of Initiation of Collision between India and Asia: A Review of Stratigraphic Data. *Earth and Planetary Science Letters*, **145**, 1-13. https://doi.org/10.1016/S0012-821X(96)00201-4

[7] Gao, X., Yin, A., Chen, B., *et al.* (2017) Oblique Stepwise Rise and Growth of the Tibet Plateau. *Nature*, **543**, 705-709.

[8] Guillot, S. and Replumaz, A. (2013) Importance of Continental Subductions for the Growth of the Tibetan Plateau. *Bulletin de la Societe Geologique de France*, **184**, 199-223. https://doi.org/10.2113/gssgfbull.184.3.199

[9] Replumaz, A., Funiciello, F., Reitano, R., Faccenna, C. and Balon, M. (2016) Asian Collisional Subduction: A Key Process Driving Formation of the Tibetan Plateau. *Geology*, **44**, 943-946. https://doi.org/10.1130/G38276.1

[10] Molnar, P. and Tapponnier, P. (1975) Cenozoic Tectonics of Asia: Effects of a Continental Collision. *Science*, **189**, 419-426. https://doi.org/10.1126/science.189.4201.419

[11] Xu, Z. Q., Jiang, M., Yang, J.S., *et al.* (2004) Mantle Structure of Qinghai-Tibet Plateau: Mantle Plume, Mantle Shear Zone and Delamination of Lithospheric Slab. *Earth Science Frontiers*, **11**, 329-343. (In Chinese)

[12] Van Hinsbergen, D.J.J., Steinberger, B., Doubrovine, P.V. and Gassmoller, R. (2011) Acceleration and Deceleration of India-Asia Convergence since the Cretaceous: Roles of Mantle Plumes and Continental Collision. *Journal of Geophysical Research*: *Solid Earth*, **116**, B06101. https://doi.org/10.1029/2010JB008051

[13] Peng, H.C., Hu, J.F., Yang, H.Y. and Badal, J. (2023) Remnants of Magma Underplating by the Emeishan Mantle Plume within the Lithosphere beneath Southeastern Margin of the Tibetan Plateau. *Tectonophysics*, **858**, Article ID: 229886. https://doi.org/10.1016/j.tecto.2023.229886

[14] Houseman, G., McKenzie, D. and Molnar, P. (1981) Convective Instability of a Thickened Boundary Layer and Its Relevance for the Thermal Evolution of Continental Convergent Belts. *Journal of Geophysical Research*: *Solid Earth*, **86**, 6115-6132. https://doi.org/10.1029/JB086iB07p06115

[15] Steinberger, B. and Calderwood, A.R. (2006) Models of Large-Scale Viscous Flow in the Earth's Mantle with Constraints from Mineral Physics and Surface Observations. *Geophysical Journal International*, **167**, 1461-1481. https://doi.org/10.1111/j.1365-246X.2006.03131.x

[16] Liu, M. and Chase, G.C. (1991) Boundary-Layer Model of Mantle Plumes with Thermal and Chemical Diffusion and Buoyancy. *Geophysical Journal International*, **104**, 433-440. https://doi.org/10.1111/j.1365-246X.1991.tb05691.x

[17] Gillian, R.F. (2010) Plates vs Plumes: A Geological Controversy. Wiley-Blackwell, Hoboken, 364 p.

[18] Molnar, P. and England, P. (1990) Late Cenozoic Uplift of Mountain Ranges and Global Climate Change: Chicken or Egg? *Nature*, **346**, 29-34. https://doi.org/10.1038/346029a0

[19] Molnar, P., Boos, W.R. and Battisti, D.S. (2010) Orographic Controls on Climate and Paleoclimate of Asia: Thermal and Mechanical Roles for the Tibetan Plateau. *Annual Review of Earth and Planetary Sciences*, **38**, 77-102. https://doi.org/10.1146/annurev-earth-040809-152456

[20] Valdiya, K.S. (1999) Rising Himalaya: Advent and Intensification of Monsoon. *Current Science*, **76**, 514-524.

[21] Molnar, P., England, P. and Martinod, J. (1993) Mantle Dynamics, Uplift of the Tibetan Plateau, and the Indian Monsoon. *Reviews of Geophysics*, **31**, 357-396. https://doi.org/10.1029/93RG02030

[22] Wang, G.C., Cao, K., Wang, A., *et al.* (2014) On the Geodynamic Mechanism of Episodic Uplift of the Tibetan Plateau during the Cenozoic Era. *Acta Geologica Sinica-English Edition*, **88**, 699-716. https://doi.org/10.1111/1755-6724.12223

[23] Bougeois, L., Dupont-Nivet, G., de Rafelis, M., *et al.* (2018) Asian Monsoons and Aridification Response to Paleogene Sea Retreat and Neogene Westerly Shielding Indicated by Seasonality in Paratethys Oysters. *Earth and Planetary Science Letters*, **485**, 99-110. https://doi.org/10.1016/j.epsl.2017.12.036

[24] Coleman, M. and Hodges, K. (1995) Evidence for Tibetan Plateau Uplift before 14-Myr Ago from a New Minimum Age for East-west Extension. *Nature*, **374**, 49-52. https://doi.org/10.1038/374049a0

[25] Zheng, B.X. (1989) Controversy Regarding the Existence of a Large Ice-Sheet on the Qinghai-Xizang (Tibetan) Plateau during the Quaternary Period. *Quaternary Research*, **32**, 121-123. https://doi.org/10.1016/0033-5894(89)90039-2

[26] Qian, W.H. and Du, J. (2023) A Study on the Plate Tectonics in the Early Earth Period Based on the Core-Magma Angular Momentum Exchange. *Open Journal of Geology*, **13**, 598-621. https://doi.org/10.4236/ojg.2023.136026

[27] You, X.T., Qian, W.H. and Zou, Y.R. (1998) A Numerical Simulation of the Effect of Global SSTA on the Low-Level Atmospheric Circulation and Precipitation Anomalies. *Acta Meteorologica Sinica*, **12**, 300-310. (In Chinese)

[28] Qian, W.H. and You, X.T. (1998) Southern Oscillation Forced by Heat Source and Topography. *Acta Oceanologica Sinica*, **20**, 33-40. (In Chinese)

[29] Qian, W.H. and Chou, J.F. (1996) Atmosphere-Earth Angular Momentum Exchange. *Science in China* (*Series D*), **39**, 215-224.

[30] Gong, H., Huang, M., Zhu, L. and Shao, Y.P. (2019) Long-Term Variations of Atmospheric Angular Momentum and Torque. *Meteorology and Atmospheric Physics*, **131**, 1697-1711. https://doi.org/10.1007/s00703-019-00663-y

[31] Zatman, S. (2001) Phase Relations for High Frequency Core-mantle Coupling and Earth's Axial Angular Momentum Budget. *Physics of the Earth and Planetary Interiors*, **128**, 163-178. https://doi.org/10.1016/S0031-9201(01)00284-9

[32] Vine, F.J. and Matthews, D.H. (1963) Magnetic Anomalies over Oceanic Ridges. *Nature*, **199**, 947-949. https://doi.org/10.1038/199947a0

[33] Gibney, E. (2022) How the Revamped Large Hadron Collider Will Hunt for New Physics. *Nature*, **605**, 604-607. https://doi.org/10.1038/d41586-022-01388-6

[34] Normile, D. and Cho, A. (2019) Physicists Brace for Decision on Japan's International Linear Collider. *Science*, **363**, 911-912.

[35] Qian, W.H. (2022) Orthogonal Collision of Particles Produces New Physical State. *Journal of Modern Physics*, **13**, 1440-1451. https://doi.org/10.4236/jmp.2022.1311089

[36] Qian, W.H. (2023) On the Physical Process and Essence of the Photoelectric Effect. *Journal of Applied Mathematics and Physics*, **11**, 1580-1597. https://doi.org/10.4236/jamp.2023.116104

[37] Qian, W.H., Leung, J.C.-H., Luo, W.M., Du. J. and Gao, J.D. (2019) An Index of Anomaly Convective Instability to Detect Tornadic and Hail Storms. *Meteorology and Atmospheric Physics*, **131**, 351-373. https://doi.org/10.1007/s00703-017-0576-z

[38] Qian, W.H., Du, J. and Ai, Y. (2021) A Review: Anomaly-Based versus Full-Field-Based Weather Analysis and Forecasting. *Bulletin of the American Meteorological Society*, **102**, E849-E870. https://doi.org/10.1175/BAMS-D-19-0297.1